Available online at www.eccomasproceedia.org
Eccomas Proceedia COMPDYN (2025) 816- 824

ECCOMAS
Proceedia

COMPDYN 2025
10th ECCOMAS Thematic Conference on
Computational Methods in Structural Dynamics and Earthquake Engineering
M. Papadrakakis, M. Fragiadakis (eds.)
Rhodes Island, Greece, 15-18 June 2025

INFLUENCE OF PILE PARAMETERS ON SEISMIC FRAGILITY ASSESSMENT OF RC BRIDGE PIER

Begum E. Ajom[1], Kaustubh Dasgupta[2], and Arindam Dey[2]

[1] Doctoral Scholar
Department of Civil Engineering, Indian Institute of Technology Guwahati, Assam, 781039, India
e-mail: begum176104101@iitg.ac.in

[2] Associate Professor, Department of Civil Engineering
Adjunct Faculty, Centre for Disaster Management and Research
Indian Institute of Technology Guwahati, Assam, 781039, India
kd@iitg.ac.in, arindam.dey@iitg.ac.in

Abstract

This study aims to develop seismic fragility curves for an RC bridge pier founded in homogenous sandy soil, incorporating the parametric influences of the pier-pile-soil interaction. Fragility analyses are conducted to assess the influence of key foundation parameters, specifically pile diameter and longitudinal reinforcement ratio, on the seismic response of the pier-pile system. A three-dimensional finite element model is developed using the Beam on Nonlinear Winkler Foundation (BNWF) approach in OpenSees, with soil behavior represented through nonlinear p–y, t–z, and Q–z springs. Incremental Dynamic Analysis is performed using a suite of 12 ground motions, and fragility curves are derived for different foundation configurations. Results indicate that foundation stiffness significantly influences damage probabilities, particularly at intermediate damage states, where stiffer foundations restrict pile yielding and concentrate nonlinearity in the pier.

Keywords: Fragility Curves, BNWF Model, IDA, RC Pier, Foundation Stiffness, Longitudinal Reinforcement Ratio, Pile Diameter, Parametric Variation

ISSN:2623-3347 Published by Eccomas Proceedia.
Peer-review under responsibility of the organizing committee of COMPDYN 2025.
doi: 10.7712/120125.1269 .25925

1 INTRODUCTION

The seismic vulnerability of RC bridge pier-pile foundation systems is influenced by structural and geotechnical factors, which govern soil-pile-structure interaction and impact bridge pier performance. While numerous studies have investigated seismic fragility analyses for bridges considering Soil-Structure Interaction (SSI) and uncertainties related to seismic hazards, the detailed effects of pile and soil parameters on the likelihood of damage in bridge piers have not been investigated in detail in the past.

Fragility curves have been used to compare modeling approaches [1] and assess parameter variations, with research highlighting SSI effects [2], pile-group fragility under flood and seismic conditions [3, 4, 5, 6], and ground motion uncertainties [7, 8]. However, the influence of structural and geotechnical parameters of bridge foundation on seismic behaviour of the pier has not been studied in detail.

The aim of the present study is to study seismic fragility of RC bridge piers on pile foundation, focusing on the influence of pile diameter and longitudinal reinforcement ratio in the piles, as these parameters are expected to significantly affect the seismic response of the pier-pile-soil system.

2 PIER-PILE-SOIL SYSTEM AND INPUT GROUND MOTIONS

In the current study, a typical pier-pile group foundation system is designed in accordance with [9, 10, 11, 12, 13]. The foundation comprises a six-pile group arranged in a 2 × 3 configuration, with each pile having a diameter of 1.2 m and a length of 25 m, embedded in homogeneous loose sand having an angle of internal friction of $29°$. The pile-cap, which monolithically connects the pier and piles, is assumed to be resting on the ground, positioning the pile-heads at the ground level. The height and the diameter of the pier are considered as 7.5 m and 2.1 m, respectively. Figure 1(a) illustrates the detailed dimensions and configuration of the pier-pile-soil system.

The grades of concrete used in pier and piles are M55 and M40, respectively. Both the pier and piles are reinforced with longitudinal steel bars having a yield strength of 500 MPa. The longitudinal reinforcement ratio is specified as 1.38% for the pier and 2% for the piles.

It is important to note that, these design values correspond to the reference case, C00, which is established based on the aforementioned Indian Standard (IS) and Indian Road Congress (IRC) guidelines. To investigate the influence of key pile parameters on the performance of the RC pier, the present study focuses on two primary variables for the piles: the longitudinal reinforcement ratio (ρ_{l_pile}) and the pile diameter (D_{pile}). While the pier parameters are kept consistent across all cases, four additional cases (C01 to C04) are created by systematically altering one parameter at a time from the reference case. Table 1 presents a summary of the parameters and their values for the five cases considered.

Case	ρ_{l_pile} (%)	D_{pile} (m)
C00 (reference)	**2**	**1.2**
C01	2	**1**
C02	2	**0.8**
C03	**1**	1.2
C04	**0.4**	1.2

Table 1: Parametric values for the considered cases in the present study.

2.1 Numerical Modelling

A three-dimensional (3D) finite element (FE) model based on the BNWF approach is developed using the open-source platform OpenSees [14] to simulate the seismic behaviour of the pier-pile group foundation system (Figure 1(b)). The pier and the piles are modeled with displacement-based beam-column elements, while the pile-cap is represented using elastic beam-column elements with very high rigidity. The superstructure mass is assigned at the pier head, and the pile-cap mass is applied at its center.

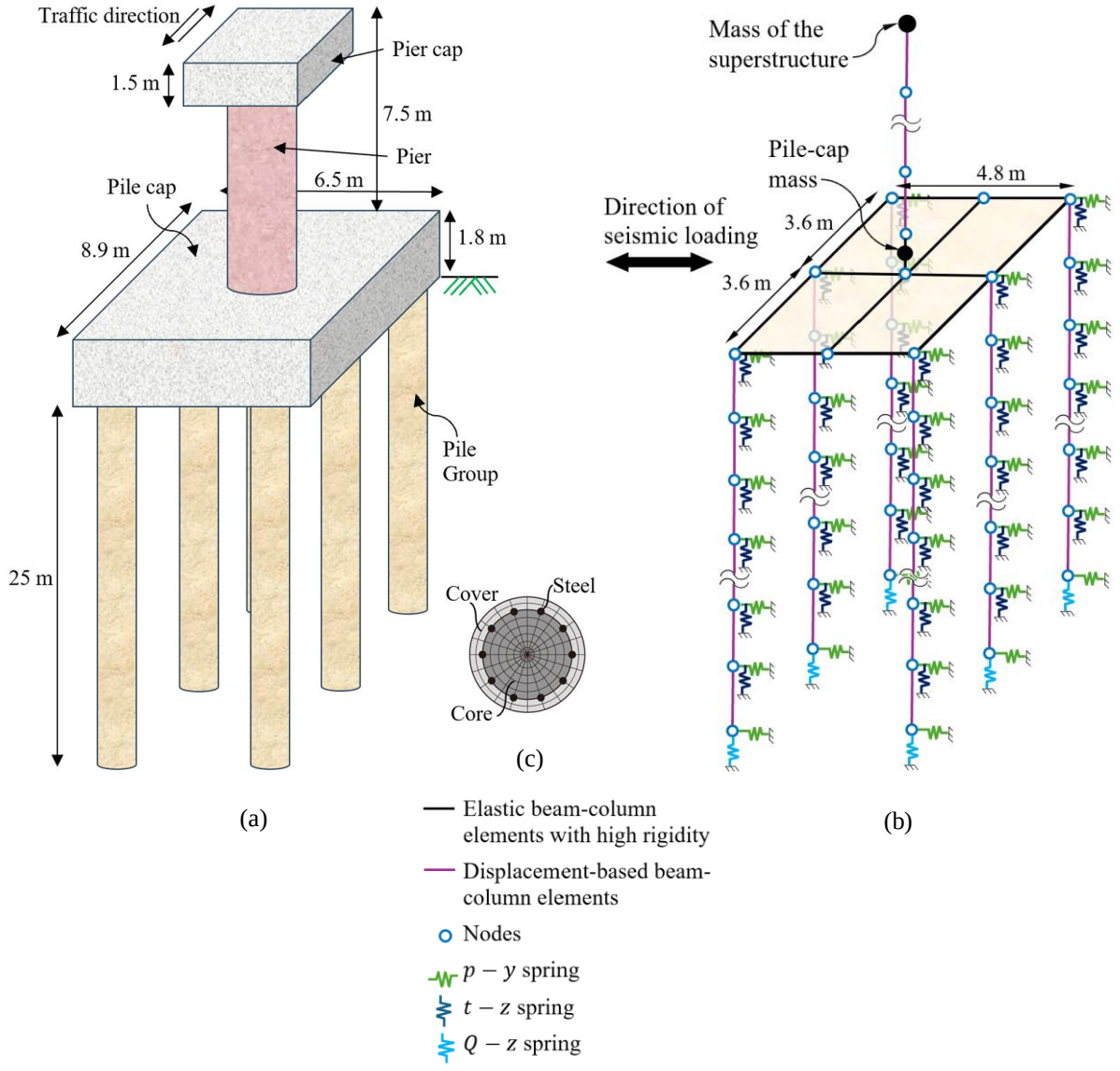

Figure 1: (a) Schematic diagram; and (b) BNWF-based FE model; of the pier-pile-soil system; (c) Fibre section.

The soil has been modelled as nonlinear springs using the *p–y*, *t-z* and *Q-z* curves representing lateral resistance, skin friction, and end-bearing resistance of the soil, respectively. Uniaxial material objects *PySimple1*, *TzSimple1* and *QzSimple1*, available in OpenSees, are assigned to the *p–y*, *t-z* and *Q-z* springs, respectively. The uniaxial material models are implemented using zero-length elements with each element connecting the pile end node and the soil end node, both located with the same spatial coordinates. In this study, the *p–y*, *t-z* and *Q-z* curves are obtained using the recommendations of [15].

The nonlinear behavior of RC pier and piles is captured using a fiber-based approach, wherein the cross-section is divided into discrete fibers, each assigned appropriate constitutive materials to represent cover concrete, core concrete, and longitudinal reinforcement (Figure 1c). The core and cover concrete fibers are modelled using *Concrete02* constitutive material, while the longitudinal reinforcement is simulated with *Steel02* material model [16]. The confined concrete properties are determined based on the relationships proposed by [17, 18].

Each pile is divided into 0.5 m long beam-column elements, with nonlinear springs attached to one end of each pile node and Displacement Time Histories (DTHs) applied at the other for seismic analysis. These displacement time histories at different depths are obtained from 1D site response analyses conducted using a 2D soil column modelled in OpenSees.

2.2 Input Ground Motions

This study selects 12 bedrock motions from the PEER Ground Motion (GM) database [19] based on magnitude (M), source-to-site distance (R), and Peak Horizontal Acceleration (PHA). The motions are categorized into:

- Sub-set 1 (low-to-moderate, far-field motions): 0 < PHA ≤ 0.4 g, M > 6, R< 12 km,
- Sub-set 2 (medium to very strong, near-field motions): 0.4 g < PHA ≤ 1.3 g, M > 6, R > 12 km.

GMs are selected at the bedrock level to ensure an unbiased representation of soil nonlinearity. Site response analyses on a homogeneous loose sand column are then conducted to generate DTHs based on the selected bedrock records. This approach provides DTHs for the BNWF model while explicitly accounting for local site conditions [2].

3 FRAGILITY ASSESSMENT METHODOLOGY

Fragility analysis is a powerful tool for assessing vulnerability, using fragility functions to estimate the probability of exceedance of pre-defined damage states. This approach links seismic demand with structural capacity to evaluate potential damage. A fragility function expresses the probability of exceeding a specific damage state for a given ground motion Intensity Measure (IM) and is typically represented by a lognormal cumulative distribution function, as described below.

$$P[D \geq C|IM] = \Phi\left(\frac{ln\left(S_D/S_C\right)}{\sqrt{\beta_{tot}^2}}\right) \tag{1}$$

where D is the demand; C is the capacity; Φ is the standard normal distribution function; S_D and S_C are median values of the demand and capacity, respectively; β_{tot} is the total uncertainty value calculated as $\beta_{tot} = \sqrt{\beta_C^2 + \beta_D^2 + \beta_{LS}^2}$, where, β_C is the uncertainty in capacity; β_D is the uncertainty in demand; β_{LS} is the uncertainty in limit state definition (for capacity thresholds).

3.1 Seismic Demand

Although various methods exist for seismic demand assessment, nonlinear time history analysis provides one of the reliable means for estimation of seismic demand. In particular, Incremental Dynamic Analysis (IDA) method is a useful method involving a suite of dynamic analyses with increasing intensity of ground motions. The present study employs IDA to evaluate the seismic demand of the pier-pile group foundation system. Selected ground mo-

tion records are scaled to different PHA levels (0.1g to 1g), with PHA as the selected IM. The scaled GM records are then applied at the base of the soil columns to perform site response analyses.

In this study, the lateral displacement at the pier head is considered as the Engineering Demand Parameter (EDP). The maximum lateral displacement at the pier head for each scaled earthquake intensity is plotted to generate an IDA curve for each GM record. The median EDP value is then computed for each IM across all GM records. This procedure is repeated for all cases listed in Table 1. Figure 2 illustrates the IDA curves of the RC pier for the reference case (C00) under 12 GMs.

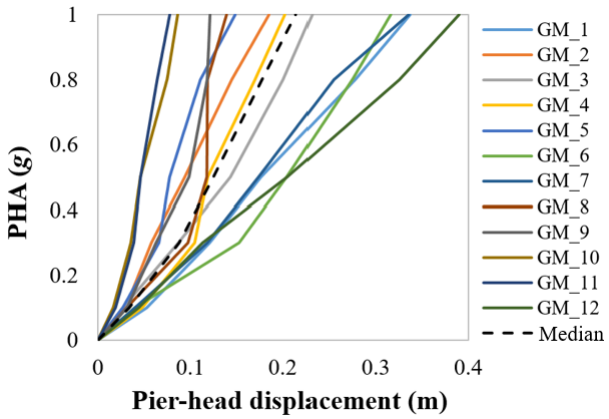

Figure 2: IDA curves of the RC bridge pier for the reference case.

3.2 Definition of Damage Limit State

As per seismic design criteria, bridge piers are allowed to undergo inelastic deformation, leading to large lateral displacements and considerable damage within plastic hinge zones. This damage initiates with concrete cracking and progresses to reinforcement yielding, concrete spalling, core concrete crushing, and reinforcement buckling [20]. The progression is directly linked to tensile and compressive strains in steel reinforcement and concrete. Damage states are typically classified qualitatively as slight, moderate, extensive, and complete [21], with quantitative strain-based limits defining these states. This study considers five damage limit states for evaluating the performance of bridge pier, as outlined in Table 2.

Damage Limit States	Damage description	Strain Limit States
DLS1: slight	First cracking of concrete	$\varepsilon_c = \varepsilon_{ctu}$
DLS2: minor	Yielding of longitudinal bar	$\varepsilon_s = \varepsilon_{sy}$
DLS3: moderate	Spalling of cover concrete	$\varepsilon_c = \varepsilon_{cu}$
DLS4: extensive	Crushing of core concrete	$\varepsilon_{cc} = \varepsilon_{ccu}$
DLS5: complete	Buckling of longitudinal bars	$\varepsilon_s = \varepsilon_{s,bb}$

Table 2: Considered damage limit states of bridge pier.

The notations in the table are described as follows: ε_c refers to the cover concrete strain, ε_{ct} represents the tensile strain of cover concrete, ε_s denotes the strain in the longitudinal bar and ε_{cc} corresponds to the strain in core concrete. The subscripts u, y and bb indicate ultimate, yield and bar buckling, respectively.

3.3 Capacity Estimation using Nonlinear Pushover Analysis

Nonlinear static pushover analyses are conducted to assess the capacity of the bridge pier for all five cases (Table 1). A displacement-controlled approach is used with the target lateral displacement as 0.5 m. Pier-head displacement is recorded for each limit state threshold, corresponding to the strain monitored at the critical section of the pier.

4 EFFECTS OF PILE PARAMETERS ON THE FRAGILITY CURVES OF PIER

The fragility curves for the RC pier, shown in Figures 3 and 4, illustrate the effects of longitudinal reinforcement ratios of piles and pile diameters, respectively. At the onset of slight damage (DLS1), corresponding to cover concrete cracking, the probability of damage remains similar for all the cases (e.g., D_{pile} = 1.2m, 1m, and 0.8m) for a particular pile parameter. This is because foundation stiffness has a more significant impact at higher damage levels when larger curvatures develop, whereas its influence is minimal in the early stages of cracking.

Figure 3 presents the probability of damage of the pier as a function of PHA across varying longitudinal reinforcement ratios in piles. Notably, higher reinforcement ratios, which increase foundation stiffness, elevate the damage probability corresponding to the yielding of longitudinal reinforcement (DLS2) and the spalling of the cover concrete (DLS3) in the pier. This occurs because stiffer foundations restrict yielding in the piles, forcing nonlinear deformation demands to the pier.

In contrast, the probabilities of severe damage states, DLS4 and DLS5, i.e., the probabilities of core concrete crushing and reinforcement buckling, remain largely unaffected by foundation stiffness. At higher damage states, the pier has already undergone significant inelastic deformation, and its residual strength is governed primarily by the inherent material properties of the concrete and steel reinforcement, rather than the flexibility of the foundation.

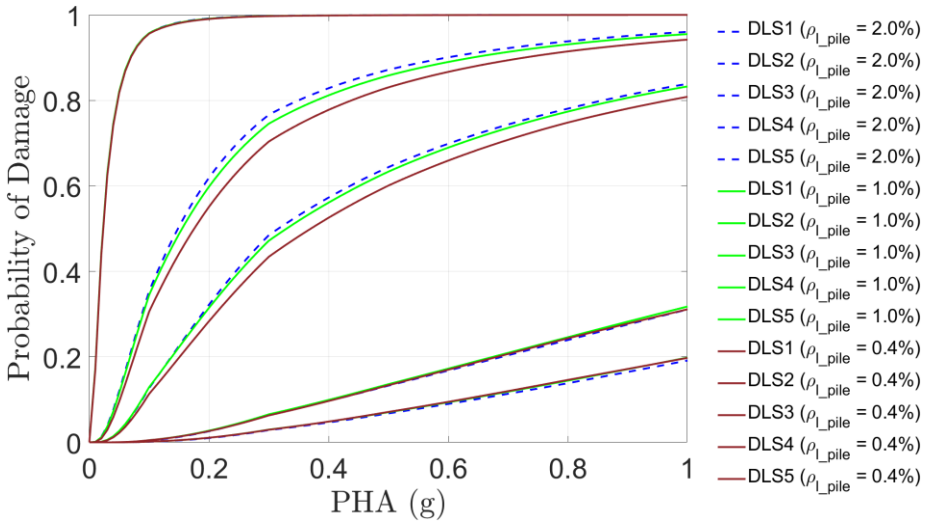

Figure 3: Fragility curves of the pier considering varying longitudinal reinforcement ratios in piles.

Figure 4 illustrates the probability of pier damage for different pile diameters. For DLS2 and DLS3, a transition phase occurs, where damage probabilities of the pier under varying pile diameters, shift as ground motion intensity increases. This is influenced by soil-pile interaction, as changes in pile diameter affect the surrounding soil volume, unlike variations in reinforcement ratio, where the surrounding soil remains unaffected.

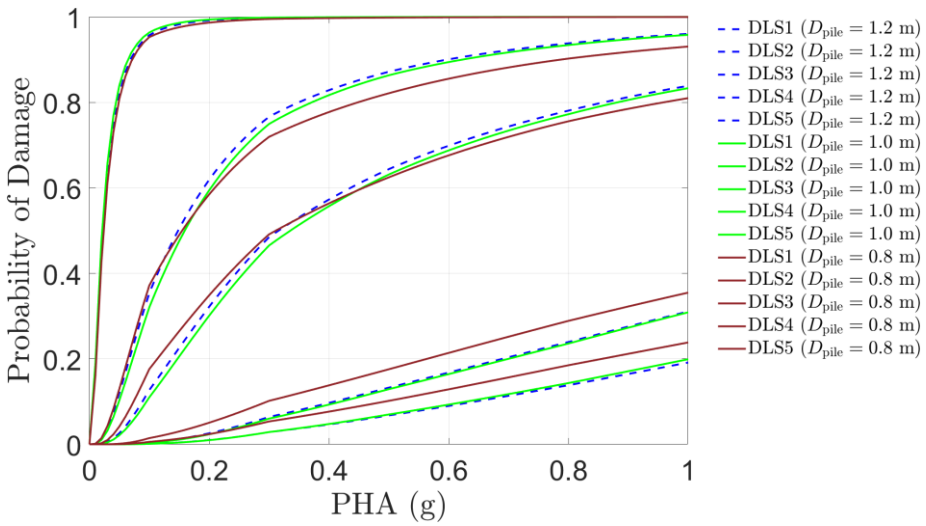

Figure 4: Fragility curves of the pier considering varying pile diameter.

With increase in pile diameter, the contact area with soil becomes large, enhancing the lateral stiffness of the foundation. At lower ground motion intensities, this increased stiffness reduces amplification, thereby lowering the probability of damage. However, at higher intensities, the stiffer system may restrict pile yielding, concentrating nonlinearity in the pier elevating its vulnerability, thereby increasing damage probability.

In contrast, smaller pile diameters result in a more flexible response due to reduced soil volume. This flexibility enables greater energy dissipation at higher intensities, reducing damage probabilities for DLS2 and DLS3. For severe damage states (DLS4 and DLS5), damage probability of pier is higher in case of flexible foundations (smaller diameter piles) and lower in case of stiffer foundations (larger diameter piles).

5 CONCLUSIONS

Seismic fragility of RC bridge piers was evaluated by incorporating pier-pile-soil interaction effects, considering variations in pile diameter and longitudinal reinforcement ratios. The salient conclusions drawn from the study are as follows:

- Foundation stiffness significantly influences damage probabilities, particularly at damage states corresponding to yielding of longitudinal reinforcements where larger curvatures start developing in the pier.
- Higher reinforcement ratios in piles increase stiffness, restricting pile yielding and concentrating nonlinearity in the pier, leading to higher damage probabilities at intermediate damage states.
- Pile diameter plays a crucial role in seismic response, with larger diameters enhancing foundation stiffness and reducing damage probability at lower intensities but increasing pier vulnerability at higher intensities.
- For severe damage states such as core concrete crushing and reinforcement buckling, foundation stiffness has minimal influence as the pier undergoes significant inelastic deformation, thereafter primarily governed by material properties.

The findings provide valuable insights for optimizing pile foundation design in seismic-prone regions, balancing stiffness and flexibility to mitigate excessive pier damage.

REFERENCES

[1] O. S. Kwon, A. S. Elnashai, Fragility analysis of a highway over-crossing bridge with consideration of soil–structure interactions. *Structure and Infrastructure Engineering*, **6(1-2)**, 159-178, 2010.

[2] S. P. Stefanidou, A. G. Sextos, A. N. Kotsoglou, N. Lesgidis, A. J. Kappos, Soil-structure interaction effects in analysis of seismic fragility of bridges using an intensity-based ground motion selection procedure. *Engineering Structures*, **151**, 366-380, 2017.

[3] X. Guo, Y. Wu, Y. Guo, Time-dependent seismic fragility analysis of bridge systems under scour hazard and earthquake loads. *Engineering Structures*, **121**, 52-60, 2016.

[4] X. Wang, A. Ye, B. Ji, Fragility-based sensitivity analysis on the seismic performance of pile-group-supported bridges in liquefiable ground undergoing scour potentials. *Engineering Structures*, **198**, 109427, 2019.

[5] R. Ghimire, P. Pradhan, D. Gautam, Multi-hazard fragility analysis of RC bridges for high seismicity and high scouring scenarios. *The Journal of Engineering*, **(6)**, 618-628, 2022.

[6] D. Zhang, W. Xiong, X. Ma, C. S. Cai, Fragility evaluation of bridge pile foundation considering scour development under floods. *Journal of Bridge Engineering, ASCE*, **29(8)**, 04024052, 2024.

[7] M. Soltani, R. Amirabadi, Seismic vulnerability assessment of pile-supported wharves using fragility surfaces. *Journal of Earthquake Engineering*, **26(14)**, 7140-7155, 2022.

[8] M. Qiu, S. Tian, L. Tang, S. Cong, X. Ling, J. Cui, Development of fragility surfaces for pile-supported structures under mainshock-aftershock sequences. *Results in Engineering*, **21**, 101826, 2024.

[9] IS 2911-1-2, *Design and construction of pile foundations, Part 1: Concrete piles, Section II: Bored Cast in-situ concrete piles*, Bureau of Indian Standards (BIS), 2010.

[10] IS 456, *Plain and reinforced concrete – Code of practice*, Bureau of Indian Standards (BIS), 2000.

[11] IRC 78, *Standard Specifications and Code of Practice for Road Bridges, Section VII, Foundations and Substructure*, Indian Road Congress, 2014.

[12] IRC 6, *Standard Specifications and Code of Practice for Road Bridges. Section II, Loads and Load Combinations*, Indian Road Congress, 2017.

[13] IRC 112, *Code of practice for concrete road bridges*, Indian Road Congress, 2020.

[14] F. McKenna, OpenSees: a framework for earthquake engineering simulation. *Computing in Science & Engineering*, **13(4)**:58–66, 2011.

[15] American Petroleum Institute (API), *Recommended practice for planning, designing, and constructing fixed offshore platforms.* API recommended practice 2A-WSD (RP 2AWSD), 21st edition, 2000.

[16] F. C. Filippou, E. P. Popov, V. V. Bertero, Effects of bond deterioration on hysteretic behavior of reinforced concrete joints. Report No. UCB/EERC-83/19, *Earthquake Engineering Research Center*, University of California, Berkeley, USA, 1983.

[17] R. Park, M. N. Priestley, W. D. Gill, Ductility of square-confined concrete columns. *Journal of the structural division, ASCE*, **108(4)**:929–950, 1982.

[18] B.D. Scott, R. Park, M.J. Priestley, Stress-strain behaviour of concrete confined by overlapping hoops at low and high strain rates. *American Concrete Institute*, **vol. 79**, no. 1, pp. 13–27, 1982.

[19] PEER Center, *Pacific Earthquake Engineering Research ground motion database*, https://ngawest2.berkeley.edu/ (accessed Feb., 2023)

[20] D. Lehman, J. Moehle, S. Mahin, A. Calderone, L. Henry, Experimental evaluation of the seismic performance of reinforced concrete bridge columns. *Journal of Structural Engineering, ASCE*, **130(6)**, 869-879, 2004.

[21] FEMA HAZUS, *Multi-hazard loss estimation methodology earthquake model: Technical manual*. Washington, DC, 2017.